USE OF IMAGE AND LASER SCANNING DATA FOR BUILDING DETECTION

Demir, N.[1], Baltsavias, E.[1]
1- (demir,manos@geod.baug.ethz.ch)
Institute of Geodesy and Photogrammetry, ETH Zurich, CH-8093, Zurich, Switzerland

KEY WORDS: DTMs/DSMs, Lidar Data Processing, Multispectral Classification, Image Matching, Information Fusion, Object Detection, Buildings

ABSTRACT:

In this work, we focus on the mainly detection of buildings.. As input data, we use LIDAR data and multispectral aerial images of two different test sites. One is from Zurich airport and the other one is from Vaihingen region close to Stuttgart. Quality assessment has been performed by comparing our results with existing reference data which are generated using commercial photogrammetric software and manual stereo measurement.

1. INTRODUCTION

In this work, we focus on the extraction of man-made structures, especially buildings and secondly trees by combining information from aerial images and Lidar data. We applied four different methods on two different dataset located at first Zurich Airport, Switzerland and secondly Vaihingen region close to Stuttgart. The first method is based on DSM/DTM comparison in combination with NDVI analysis; in case of lacking DTM, a slope based morphological filter has been used to detect all the off-terrain objects which include buildings, trees and other objects. The second one is a supervised multispectral classification refined with height information from Lidar data. The third approach uses voids in Lidar DTM and NDVI classification, while the last method is based on the analysis of the density of the raw Lidar DSM data. The accuracy of the building extraction process was evaluated by comparing the results with reference data and computing the percentage of data correctly extracted and the percentage of missing reference data. The improvement of the result has been performed by taking into account the advantages and disadvantages of each method. For extraction of 3D surfaces, a RANSAC method has been applied to find all planar surfaces which belong to the roof surfaces. Quality assessment has been performed by comparing our results with existing vector reference data.

2. PREVIOUS WORK

Aerial images and Lidar data are common sources for object extraction. In digital photogrammetry, features of objects are extracted using 3D information from image matching or DSM/DTM data, spectral, textural and other information sources. Pixel-based classification methods, either supervised or unsupervised, are mostly used for land-cover and man-made structure detections. For the classical methods e.g. minimum-distance, parallelepiped and maximum likelihood, detailed information can be found in (Lillesand and Kiefer, 1994).

In general, the major difficulty in using aerial images is the complexity and variability of objects and their form, especially in suburban and densely populated urban regions (Weidner and Foerstner, 1995).
Regarding object extraction from LIDAR data, it has been defined as a filtering problem of the DSM (raw or interpolated) data by several researches. Some algorithms use raw data (Sohn and Dowman, 2002; Roggero, 2001; Axelsson, 2001; Vosselman and Maas, 2001; Sithole, 2001; Pfeifer et al., 1998), while others use interpolated data (Elmqvist et al., 2001; Brovelli et al., 2002; Wack and Wimmer, 2002).

To detect roof structures, surface segmentation techniques are needed. The mostly used methods are based on region growing (Rabbani et al., 2006; Tovari , 2006; Gorte 2002), model fitting such as Hough Transform (Maas and Vosselman, 1999; Vosselman, 2004), RANSAC method (Schnabel et.al, 2007a; Schnabel et al., 2007 b; Bretar and Roux, 2005; Tarsha Kurdi 2007). On the other hand, Sapkota (2008) segments the colored point cloud data which have color information using Hough transform and color information when it is available.

In general, in order to overcome the limitations of image-based and Lidar-based techniques, it is of advantage to use a combination of these techniques. Sohn and Dowman (2007) used IKONOS images to find building regions before extracting them from Lidar data. Straub (2004) combines information from infrared imagery and Lidar data to extract trees. Rottensteiner et al. (2005) evaluate a method for building detection by the Dempster-Shafer fusion of Lidar data and multispectral images. They improved the overall correctness of the results by fusing Lidar data with multispectral images.

Few commercial software packages allow automatic terrain, tree and building extraction from Lidar data. In TerraSCAN, a TIN is generated and progressively densified, the extraction of off-terrain points is performed using the angles between points to make the TIN facets and the other parameter is the distance to nearby facet nodes (Axelsson, 2001). In SCOP++, robust methods operate on the original data points and allow the simultaneous elimination of off-terrain points and terrain surface modelling (Kraus and Pfeifer, 1998).

In summary, most approaches try to find objects using single methods. In our strategy, we use different methods using all available data with focus on improving the results of one method by exploiting the results from the remaining ones.

3. INPUT DATA AND PREPROCESSING

We have two different datasets. One is from Zurich Airport area, the other one is from Vaihingen region close to Stuttgart.

3.1 Zurich Airport

For the Zurich Airport area, RGB and CIR images, LIDAR raw and interpolated DSM and DTM data and 3D vector data are available. Vector data has only been used for quality assessment purposes. The 3D vector data describe buildings (including airport parking buildings and airport trestlework structures)

with 20 cm vertical accuracy. It has been produced semi-automatically from stereo aerial images using the commercial software CC-Modeler (Gruen and Wang, 1998).

Analogue RGB and CIR images were acquired with the characteristics given in Table 1.

Image Data	**RGB**	**CIR**
Acquisition Date	July 2002	July 2002
Ground Sampling Distance (GSD) (cm)	14.5 cm	8.7 cm
Lidar Data	**DSM**	**DTM**
Provider	Swisstopo	Swisstopo
Type	Raw & grid	Raw & grid
Raw point density & Grid Spacing	1 pt / 2 sqm & 2m	1 pt / 2 sqm & 2m
Acquisition Date	Feb. 2002	Feb. 2002
Vector data	Only for validation purposes	
Provider	Unique Co.	
Horizontal / Vertical Accuracy (2 sigma)	20 / 25 cm	

Table 1. Input data characteristics (Zurich Airport).

The images have been first radiometrically preprocessed (noise reduction and contrast enhancement), then the DSM was generated with the software package SAT-PP, developed at the Institute of Geodesy and Photogrammetry, ETH Zurich (Zhang, 2005).The NIR band was selected for DSM generation. The final DSM was generated with 50cm grid spacing. Using this DSM, CIR orthoimages were produced with 12.5cm ground sampling distance.

Lidar raw data (DTM-AV and DSM-AV) have been acquired with "leaves off" in February 2002 by Swisstopo. The DSM-AV point cloud includes all Lidar points (including points on terrain, tree branches etc.) and has an average point density of 1 point per 2 m^2. The DTM-AV data includes only points on the ground, so it has holes at building positions and less density at tree positions. The height accuracy (one standard deviation) is 0.5 m generally, and 1.5 m at trees and buildings. The 2m spacing grid DSM and DTM were generated by Swisstopo with the Terrascan commercial software from the original raw data.

3.2 Vaihingen Region

For the Vaihingen area, the dataset have been provided from DGPF camera evaluation project. We have used ADS-40 digital images, LIDAR raw DSM data and an image based DSM (Wolff, 2009) which has been generated using DMC images with SAT-PP and a grid spacing is 20 cm.. In this dataset, a DTM data is not available and the reference vector data has been generated with 2D manual measurement using orthophoto.. Input data characteristics can be seen in Table 2.

Data	**GSD**	**Acquisition Date**
DMC	8 cm.	24.07.2008 / 06.08.2008
ADS-40	8cm.	06.08.2008
LIDAR	5 pts / m2	21.08.2008

Table 2. Input data characteristics (Vaihingen region).

4. BUILDING DETECTION

Four different approaches have been applied to exploit the information contained in the image and Lidar data, extract different objects and finally buildings. The first method is based on DSM/DTM comparison in combination with NDVI (Normalised Difference Vegetation Index) analysis for building detection. For Vaihingen area, while there is no available DTM data, a morphological filtering approach (Zhang, et.al.,2003). has been applied to detect off-terrain objects. The second approach is a supervised multispectral classification refined with height information from Lidar data and image-based DSM. The third method uses voids in Lidar DTM and NDVI classification. The last method is based on the analysis of the density of the raw DSM Lidar data. The accuracy of the building detection process was evaluated by comparing the results with the reference data and computing the percentage of data correctly extracted and the percentage of reference data not extracted.

4.1 DSM/DTM and NDVI (Method 1)

The above-ground objects have been detected by subtracting the DTM from the DSM, the blobs include mainly buildings and trees. As DSM, the surface model generated by SAT-PP and as DTM the Lidar DTM grid were used. A standard unsupervised (ISODATA) classification of the CIR orthoimage was used to compute an NDVI image, containing vegetation (mainly trees and grass). The intersection of the nDSM with NDVI corresponds to trees. By subtracting the resulting trees from the blobs, the buildings are obtained. 83% of building class pixels were correctly classified, while 7% of the reference data were not detected. In the final result, some non-building objects are remaining such as aircrafts and vehicles. The extracted buildings are shown in Figure 1.

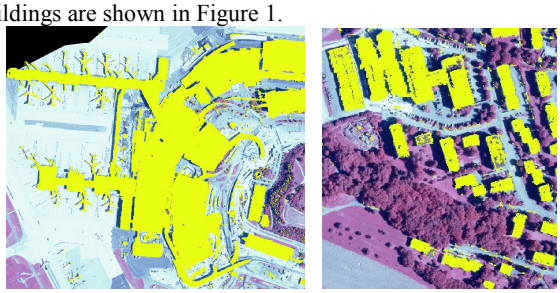

Figure 1. Building detection result from method 1. (Left: airport buildings, Right: residential area).

4.1.1 In Case of Lacking input DTM

In our second dataset, there is no input DTM available, and so an filtering approach has been needed for the DSM.

A progressive morphological filtering method has been used for blob detection. For the filtering approach, an input interpolated image based DSM data has been used. Then a morphological filter has been used to detect the off-terrain objects (Fig. 2) which include buildings, trees and other objects. We perform an opening (erosion + dilation) operation on the interpolated surface to derive a secondary surface. The elevation difference of a grid between the previous and current surface is compared to a threshold to determine if the grid is a non-ground measurement. The height difference threshold (dh) has been computed using the predefined maximum terrain slope(s). The size of filtering windows (w) has been increased and the derived surface has been used as an input for the next operation (Zhang et al., 2003).

· $dh=s(w_i-w_{i-1})c+dh_0$
If $dh>dh_{max}$ $dh=dh_{max}$

dh is the height difference threshold
dh_0 is the initial elevation difference threshold which approximates the error of DSM measurements (0.2-0.3 m),
dh_{max} is the maximum elevation difference threshold (m)
c is the grid size (m)
s is the predefined maximum terrain slope (percent slope)
wi is the filtering window size (in number of cells) at ith iteration.

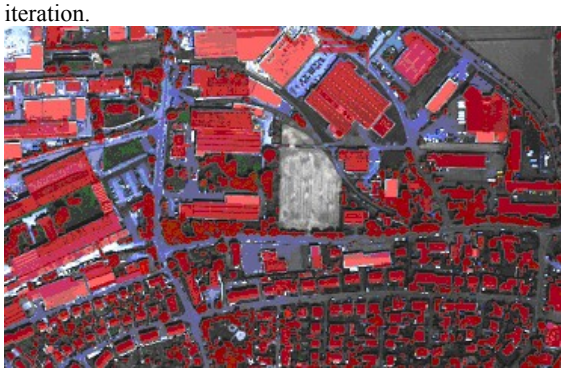

Figure 2.The detected off-terrain objects (mainly buildings and trees) after filtering

After detection of the blobs for Vaihingen dataset, vegetated regions have been detected by unsupervised classification of NDVI image, after removal of tree regions from the blobs, the buildings have been detected (Fig. 3). After the quality analysis with the reference data, the correctness has been calculated as 82% and the ommision error is 13%. The errors occur mainly by the shadow regions on vegetated areas, and on the other the reference data may contain errors since it has been generated using ortoimage by manual measurements.

Figure 3.The detected buildings after elimination of the trees

4.2 Supervised classification and use of nDSM (Method 2)

The basic idea of this method is to combine the results from a supervised classification with the height information contained in the blobs. Supervised classification methods are preferable to unsupervised ones, because the target of the project is to detect well-defined standard target classes (airport buildings, bare ground, grass, trees, roads, residential houses, shadows etc.), present at airport sites. The training areas were selected manually using AOI (Area of Interest) tools within the ERDAS Imagine commercial software (Kloer, 1994). Among the available image bands for classification (R, G and B from colour images and NIR, R and G bands from CIR images), only the bands from CIR images were used due to their better resolution and the presence of NIR channel (indispensable for vegetation detection). In addition, new synthetic bands were generated from the selected channels: a) 3 images from principal component analysis (PC1, PC2, PC3); b) one image from NDVI computation using the NIR-R channels and c) one saturation image (S) obtained by converting the NIR-R-G channels in the IHS (Intensity, Hue, Saturation) colour space.
The combination NIR-R-PC1-NDVI -S was selected for classification using separability analysis. The maximum likelihood classification method was used. As expected from their low values in the divergence matrix, grass and trees, airport buildings and residential houses, airport corridors and bare ground, airport buildings and bare ground could not be separated. Using the height information from the blobs, airport ground and bare ground and roads were fused into “ground” and airport buildings with residential houses into “buildings”, while trees and grass, as well as buildings and ground could be separated. The final classification is shown in Figure 2. 84% of the building class is correctly classified, while all of 109 buildings have been detected but not fully, the omission error is 9% . Aircrafts and vehicles are again mixed with buildings (Fig. 4).

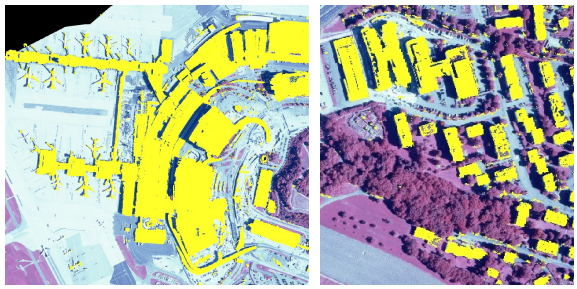

Figure 4. Building detection result from method 2. (Left: airport buildings, Right: residential area).

For Vaihingen region (Fig. 5), ADS-40 images have been used and produced an orthophoto has been generated using existing Lidar DSM, the same channels have been selected as at the Zurich airport region. After the quality analysis with the reference data, the correctness has been calculated as 86% and the ommision error is 15%.

Figure 5. Building detection result from method 2 (Vaihingen).

4.3 Building detection using density of raw Lidar DTM and NDVI (Method 3)

Buildings and other objects, like high or dense trees, vehicles, aircrafts, etc. are characterized by null or very low density in the DTM point cloud. Using the vegetation class from NDVI channel as a mask, the areas covered by trees are eliminated, while small objects (aircrafts, vehicles) are eliminated by deleting them, if their area is smaller than $25m^2$. Thus, only

buildings remain (Figure 6). 85% of building class pixels are correctly classified, while 108 of 109 buildings have been detected but not fully extracted, the omission error is 8% .

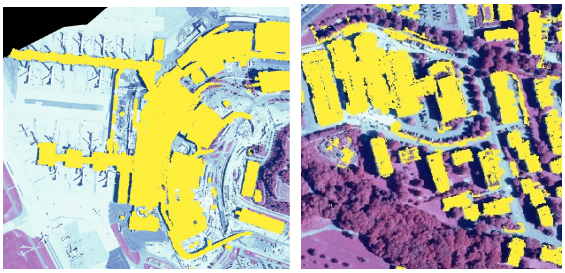

Figure 6. Building detection result from method 3. (Left: airport buildings, Right: residential area).

Since have DTM raw point cloud is not available for Vaihingen region, this method could not be applied and analyzed.

4.4 Building and tree detection from Lidar data (Method 4)

As mentioned above, in the raw DSM data the point density is generally much higher at trees than at open terrain or buildings. On the other hand, tree areas have low horizontal point density in the raw DTM data. We start from regions that are voids or have low density in the raw DTM (see Method 3), for the second dataset, we have used Lidar points in the blobs which from the filtering process, and in the next step, we used a search window over the raw Lidar DSM data with a size of 5 m x 5 m. Neighboring windows have an overlap of 50%. The window size has a relation with the number of points in the window and the number of the points in the search window affects the quality of the detection result. The method uses all points in the window and labels them as tree if all parameters below have been met. The size of $25m^2$ has been agreed to be enough to extract one single tree. A bigger size may result in wrong detection especially in areas where the buildings are neighboring with single trees.

The points in each search window are projected onto the xz and yz planes and divided for each projection in eight equal sub-regions using x_{min}, x_{mid}, x_{max}, z_{min} z_{mid1} z_{mid2} z_{mid3} z_{max} as boundary values of sub-regions, with $x_{mid} = x_{min} + 2.5m$, $x_{max} = x_{mid} + 2.5m$, $z_{mid1}=z_{min}+(z_{max}-z_{min})/4$, $z_{mid2} =z_{min}+2*(z_{max}-z_{min})/4$, $z_{mid3}=z_{min}+3*(z_{max}-z_{min})/4$ and similarly for the yz projection. The density in the eight sub-regions is computed. The first step is the detection of trees and the second the subtraction of tree points from all off-terrain points. The parameters have been calculated using tree-masked areas of the raw Lidar DSM data. The tree mask has been generated by Method 2.

The trees have been extracted by four different parameters. The first parameter (s) is similarity of surface normal vectors. We assume that the tree points would not fit to a plane. With selection of three random points in the search window, the surface normal vectors have been calculated n (number of points in search window) times. Then, all calculated vectors have been compared among each other. In case of similar value of compared vectors, the similarity value was increased by adding 1. In the tree masked points, the parameter (s) has been calculated as smaller than 2. The second parameter (vd) is the number of the eight sub-regions which contain at least one point. The trees have high Lidar point density vertically. Thus, at trees more sub-regions contain Lidar points. Using the tree mask, we have observed that at least 5 out of the 8 sub-regions contain points. Thus, the parameter (vd) has been selected as vd>4. The third parameter (z) is the tree height. Using the tree mask from multispectral classification, we calculated the minimum tree height as 3m. The fourth parameter (d) is the point density. The minimum point density has been calculated for the tree masked areas as 20points/ $25m^2$. By applying these four parameters to the raw DSM Lidar data, the tree points (Fig. 8) have been extracted and eliminated from all off-terrain points to extract the buildings. The workflow can be seen in Figure 7.

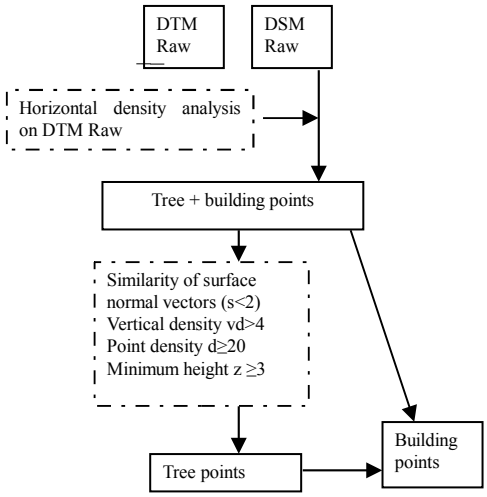

Figure 7. Workflow of detection of buildings in method 4 (Zurich Airport)

Figure 8. Detected trees in method 4 (Zurich Airport)

The density of point cloud directly affects the quality of the result. In addition, some tree areas could not be extracted because of the low point density of the Lidar data. The accuracy analysis shows that 84% of buildings area are correctly extracted, while 100 of 109 buildings have been detected but not fully extracted, the omission error is 17% . (Figure 9).

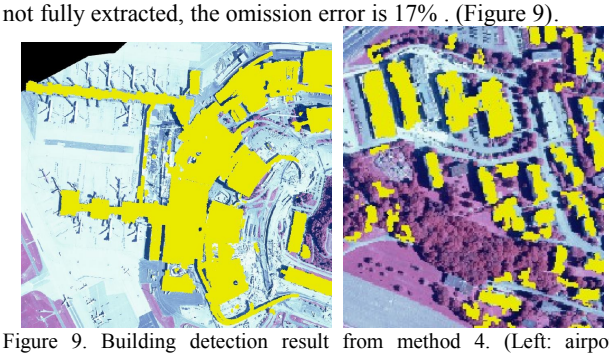

Figure 9. Building detection result from method 4. (Left: airport buildings, Right: residential area).

For the Vaihingen region, similar approach has been applied, except the result from morphological filtering has been used as an input (Fig 10).

Figure10. Building detection result from method 4(Vaihingen)

5. ANALYSIS OF THE RESULTS

Each method shows similar performance with differences in completeness. The improvement of the results is performed by taking into account the advantages and disadvantages of the methods.

For Zurich dataset, regarding completeness, the reference data has been generated using aerial images, and some buildings are in construction process. In the construction areas, these buildings were measured as fully completed, although they were only partly constructed in reality. On the other hand, due to the temporal difference between the reference vector and Lidar data, the completeness of Lidar-based methods (methods 3 and 4) has also been negatively affected.

(1∩2): While method 2 does not contain shadow on vegetation, intersection of these two methods eliminates the problems from shadow on-vegetation. The correctness of the extracted buildings from this combination is 86%, and the omission error is 12%.

(1∩2) ∩4: This combination eliminates the airplane objects from the extraction result (Figure 11). The other advantage of this combination is that it eliminates the problems which come from the construction process on some buildings. The correctness of the extracted buildings from this result is 84%, and the omission error is 8%.

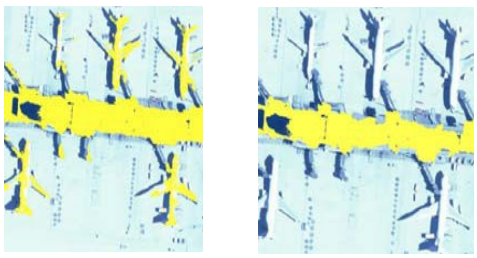

Figure 11 Left: Airplanes which were detected as buildings in (1∩2), Right: Elimination of airplanes with (1∩2) ∩4.

((1∩2) ∩4) U **3**: combination eliminates the errors resulted by the shadow on vegetation, the airplane objects, shadow regions (Fig. 12).

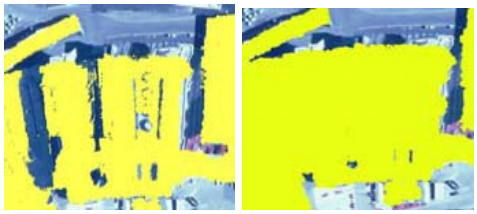

Figure 12. Left: buildings without the regions which covered by shadow in ((1∩2) ∩4), Right: more complete roofs with ((1∩2) ∩4) U 3.

After the quality analysis with the reference data, the correctness has been calculated as 91% and the omission error is 7%. More details can be found in (Demir et al, 2009)

Shadow related errors have also been seen in the results of Vaihingen dataset. While the result from method 3 is not available, only ((1∩2) ∩4) combination has been done. The result of this combination contains the regions which are in the results of the all methods, so the result is expected to be more accurate but less complete. After the quality analysis with the reference data, the correctness has been calculated as 88% and the omission error is 17%. The later approach which is detection of roof surfaces will eliminate the non-building objects.

6. ROOF SURFACE DETECTION AND GENERATION OF FINAL BUILDING POLYGONS

Detection of roof surfaces has been followed after detection of the building polygons. We have aimed to extract roof surfaces and improved the quality of detection result with elimination of points which don't belong to roof surfaces. First, raw LIDAR data have been overlaid on the detection result and later roof surface extraction process have been applied. Before that, 2 m. dilation has been applied to take more Lidar points as much as possible which belong to the roof surfaces (Fig 14).

Schnabel (2007a) and Schnabel et al., (2007b)'s RANSAC method has been used for fitting of the roof surfaces into geometrical models mainly planes. RANSAC generates a large amount of hypothesis of primitive shapes by randomly selecting minimum subset of sample points that each uniquely determines the parameter of a primitive.

The scoring mechanism is employed to detect the best primitive. The process starts with calculating the surface normal vectors of each point with selection of neighboring points. The localized sampling strategy has been used by octree data structure for the random selection of minimal subset of points in this method.

The score of the candidate shape is evaluated by using the parameters which are the tolerance distance of shape, minimum deviation of surface normal and connectivity of points. After detection of the points which belong to roof surfaces, all other points, which don't belong to any geometrical shape, have been removed, and new building polygons have been generated to improve the detection accuracy (Fig 13-15). Quality assessment of the plane detections has been performed qith visual check for only the residential buildings of Zurich dataset since the reference data for roof planes do not exist for Vaihingen dataset and not reliable for airport terminal buildings. Within the selected area, 99 roof planes were visually identified and labeled by the reference vector data. Detection process has

given 113 planes for the selected area. 14 planes have not been correctly detected, they are mostly small plane detections which should already belong to other plane surfaces.

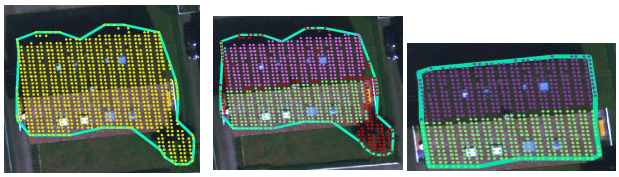

Figure 13. Left:detected building outline(cyan) and LIDAR points(yellow), Middle:detected roof plane points(purple-green) and non-roof points (red), Right:New building outline after elimination of non- roof points

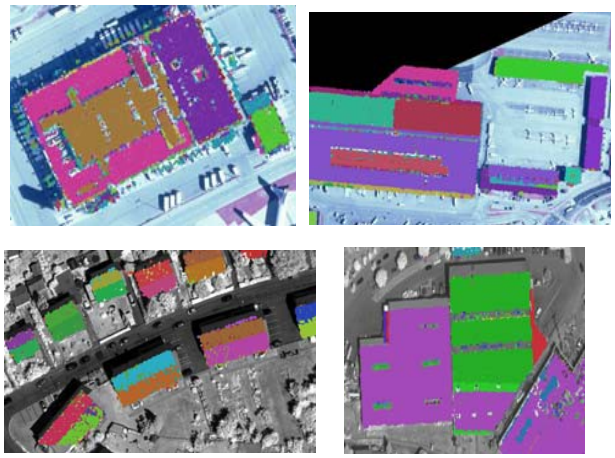

Figure 14 .Some examples from extracted roof segments (up:Zurich airport, down: Vaihingen)

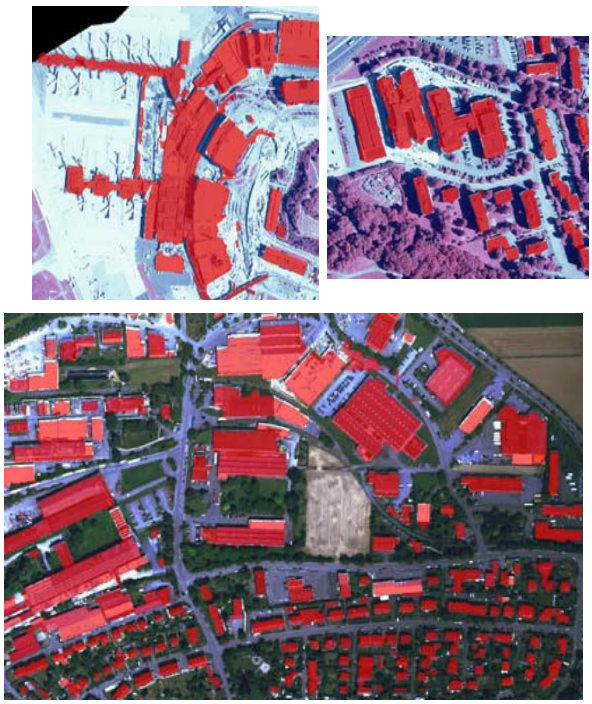

Figure 15 .Final building polygons (up: Zurich airport, down: Vaihingen)

7. CONCLUSIONS AND FUTURE WORK

In this paper, different methods for object detection (mainly buildings) in Lidar data and aerial images have been presented. In each method, the basic idea was to get first preliminary results and improve them later using the results of the other methods. The methods have been tested on two dataset located at Zurich Airport, Switzerland, and Vaihingen region, Germany.

The results from each method have been combined according to their error characteristics. Roof surfaces have been extracted and finally, the correctness of detection has been improved to 94% with remaining 7% omission error for Zurich airport, and 90% with remaining 17% omission error for the Vaihingen dataset. Further processes will be applied for the quality assessment of the detected roof planes and then direct 3D edge matching will be done and detection of 3D inner and outlines using aerial images will be generated. First 2D line segments will be extracted using Harris corner and canny edge detectors with splitting edges in Harris corner points. Then 2D line matching will be performed to reconstruct 3D lines. After extraction of 3D lines, reconstruction of roofs will be completed by combination of 3D roof surfaces and 3D lines of the roofs. This combination will be done with grouping of 3D lines according to their 3D surfaces.

ACKNOWLEDGEMENTS

This work has been supported by the EU FP6 project Pegase and KTI. We acknowledge data provided by Swisstopo and Unique Company (Airport Zurich), DGPF and we would like to thank Mr.Schnabel from University of Bonn, to provide us the algorithm library for the RANSAC approach.

REFERENCES

Axelsson, P., 2001. Ground estimation of laser data using adaptive TIN-models. Proc. of OEEPE workshop on airborne laserscanning and interferometric SAR for detailed digital elevation models, 1-3 March, Stockholm, Sweden, pp. 185-208.

Brovelli, M.A., Cannata, M., Longoni U.M., 2002. Managing and processing Lidar data within GRASS. Proc. of the GRASS Users Conf. 2002, Trento, Italy. http://citeseer.ist.psu.edu/541369.html (accessed 02 July 2009).

Demir, N., Poli, D., Baltsavias, E., 2009.Detection of Buildings at Airport Sites Using Images & Lidar Data and a Combination of Various Methods, IAPRS, Vol. 38, Part 3/W4, pp 71-77, Paris-France.

Elmqvist, M., Jungrt, E., Lantz, F., Persson, A., Soderman, U., 2001. Terrain modeling and analysis using laser scanner data. IAPRS*, Vol. 34, Part 3/W4, pp. 219-227. http://www.isprs.org/commission3/annapolis/pdf/Elmqvist.pdf (accessed 02 July 2009).

Gorte, B., 2002. Segmentation of tin-structured surface models, Joint Conference on Geo-spatial theory, Processing and Applications, Ottawa, Canada, 8-12 July
http://academics.ewi.tudelft.nl/live/binaries/2faaf567-465a-48c7-b204-4944195b6b6c/doc/BenSegmentOtowa.pdf

Gruen, A., Wang, X., 1998. CC-Modeler: A topology generator for 3-D city models. ISPRS Journal of Photogrammetry & Remote Sensing 53(5), 286-295. http://linkinghub.elsevier.com/retrieve/pii/S0924271698000112 (accessed 02 July 2009).

Kloer, B. R., 1994. Hybrid parametric/non-parametric image classification. Paper presented at the ACSM-ASPRS Annual Convention, Reno, Nevada, April. http://libraries.maine.edu/Spatial/gisweb/spatdb/acsm/ac94035.html (accessed 02 July 2009).

Kraus, K., Pfeifer, N., 1998. Determination of terrain models in wooded areas with airborne laser scanner data. ISPRS Journal of Photogrammetry & Remote Sensing 53(4) ,193-203.http://linkinghub.elsevier.com/retrieve/pii/S0924271698000094 (accessed 02 July 2009).

Lillesand, M.,Tt., Kiefer, W., R., 1994. Remote Sensing and Image Interpretation, Third Edition, John Wiley & Sons, Inc., New York, 750 pp.

Maas, H-G., Vosselman, G., 1999. Two algorithms for extracting building models from raw laser altimetry data. ISPRS Journal of Photogrammetry and Remote Sensing. 54(2-3).pp.153-163.

Pegase, 2009. http://dassault.ddo.net/pegase (accessed 27 June 2009).

Pfeifer, N., Kostli, A., Kraus, K., 1998. Interpolation and filtering of laser scanner data - implementation and first results. International Archives of Photogrammetry Vol. 32, Part 3/1, pp. 153 - 159.

Rabbani, T., van den Heuvel, F.A., Vosselman, G., 2006. Segmentation of point clouds using smoothness constraints. IAPRS*, vol. 36, part 5, Dresden, Germany, pp..248-253.

Roggero, M., 2001. Airborne Laser Scanning: Clustering in raw data. IAPRS*, Vol. 34, Part 3/W4, pp. 227-232. http://www.isprs.org/commission3/annapolis/pdf/Roggero.pdf (accessed 02 July 2009).

Rottensteiner, F., Trinder, J., Clode, S., Kubik, K., 2005. Using the Dempster Shafer method for the fusion of LIDAR data and multi-spectral images for building detection. Information Fusion 6 (4), 283–300. http://linkinghub.elsevier.com/retrieve/pii/S1566253504000466 (accessed 02 July 2009).

Sapkota, P., 2008. Segmentation of Coloured Point Cloud Data. MSc Thesis, ITC. Enchede, The Netherlands. http://www.itc.nl/library/papers_2008/msc/gfm/sapkota.pdf(accessed 01 April 2010).

Schnabel, R., Wahl, R., Klein, R., 2007a. Efficient RANSAC for Point-Cloud Shape Detection. Computer Graphics Forum. 26(2). pp.214-226 http://cg.cs.uni-bonn.de/aigaion2root/attachments/schnabel-2007-efficient.pdf (accessed 01 April 2010).

Schnabel, R., Wahl, R., Wessel, R., Klein, R., 2007b. Shape Recognition in 3D Point Clouds. Computer Graphics Technical report, No : CG-2007-1, University of Bonn, Germany, http://cg.cs.uni-bonn.de/aigaion2root/attachments/cg-2007-1.pdf (accessed 01 April 2010).

Sithole, G., 2001. Filtering of laser altimetry data using a slope adaptive filter. IAPRS*, Vol. 34, Part 3/W4, pp. 203-210.http://www.isprs.org/commission3/annapolis/pdf/Sithole.pdf (accessed 02 July 2009).

Sohn, G., Dowman, I., 2002. Terrain surface reconstruction by the use of tetrahedron model with the MDL criterion. IAPRS*, Vol. 34, Part 3A, pp. 336-344. http://www.isprs.org/commission3/proceedings02/papers/paper137.pdf (accessed 02 July 2009).

Sohn, G., Dowman, I., 2007. Data fusion of high-resolution satellite imagery and LiDAR data for automatic building extraction. ISPRS Journal of Photogrammetry and Remote Sensing 62(1), 43-6. http://dx.doi.org/10.1016/j.isprsjprs.2007.01.001 (accessed 02 July 2009).

Straub, B.-M., 2004. A multiscale approach for the automatic extraction of tree tops from remote sensing data. IAPRS*, Vol. 35, Part B3, pp. 418-423. http://www.cartesia.org/geodoc/isprs2004/comm3/papers/306.pdf (accessed 02 July 2009).

Tarsha-Kurdi, F., Landes, T., Grussenmeyer, P., 2007. Hough-transform and extended RANSAC algorithms for automatic detection of 3D building roof planes from Lidar data. IAPRS*, Vol. 36, Part 3/ W52. pp.407-412. http://www.commission3.isprs.org/laser07/final_papers/Tarsha-Kurdi_2007.pdf (accessed 02 July 2009).

Tovari, D., 2006. Segmentation Based Classification of Airborne Laser Scanner Data. PhD Thesis, Universität Karlsruhe, Karlsruhe, Germany. http://digbib.ubka.uni-karlsruhe.de/volltexte/documents/3278 (accessed 15 May 2009).

Vosselman, G., Maas, H., 2001. Adjustment and filtering of raw laser altimetry data. Proc. of OEEPE workshop on airborne laserscanning and interferometric SAR for detailed digital elevation models, 1-3 March, pp.62-72. http://www.tudresden.de/ipf/photo/publikationen/aeltere/Vosselmann_Maas_OEEPEStockholm2001.pdf (accessed 02 July 2009).

Vosselman, G., Gorte, B., Sithole, G., Rabbani, T., 2004. Recognizing structure in laser scanning point clouds. IAPRS, vol 36, part 8/W2, Freiburg, Germany, pp.33-38 http://citeseerx.ist.psu.edu/viewdoc/download?doi=10.1.1.118.6228&rep=rep1&type=pdf (accessed 10 May 2010).

Wack R., Wimmer A., 2002. Digital Terrain Models from Airborne Laser Scanner data – A grid based approach. IAPRS*, Vol 34, Part 3B, pp. 293-296.

Weidner, U., Foerstner, W., 1995. Towards automatic building extraction from high-resolution digital elevation models. ISPRS Journal of Photogrammetry and Remote Sensing 50(4), pp.38 - 49. http://linkinghub.elsevier.com/retrieve/pii/092427169598236S (accessed 02 July 2009).

Wolff, K., 2009.DGPF Project: Evaluation of digital photogrammetric aerial based imaging systems – generation of digital surface models. ISPRS Hanover Workshop 2009, "High Resolution Earth Imaging for Geospatial Information", Hanover, Germany.

Zhang, K., Chen, S., Whitman, D., Shyu, M., Yan, J.,Zhang, C., 2003. A progressive morphological filter for removing non-ground measurements from airborne LIDAR data. IEEE Transactions on Geoscience and Remote Sensing, 41,pp. 872-882. http://users.-cis.fiu.edu/~chens/PDF/TGRS.pdf

Zhang, L., 2005. Automatic Digital Surface Model (DSM) generation from linear array images. Ph.D. thesis, Institute of Geodesy and Photogrammetry, ETH Zurich, Report No. 90. http://e-collection.ethbib.ethz.ch/show?type=diss&nr=16078 (accessed 02 July 2009).

* IAPRS: International Archives of The Photogrammetry, Remote Sensing and Spatial Information Sciences